ornl

ORNL/ATD-50

OAK RIDGE NATIONAL LABORATORY

MARTIN MARIETTA

DEVELOPMENT OF SENSORS FOR CERAMIC COMPONENTS IN ADVANCED PROPULSION SYSTEMS

D. L. Beshears
M. L. Bridges
G. J. Capps
T. L. Hatmaker
H. M. Henson
T. J. Henson
B. S. Lankford
R. S. Sadler-Sherles
L. A. Zevenbergen

November 1990

MANAGED BY
MARTIN MARIETTA ENERGY SYSTEMS, INC.
FOR THE UNITED STATES
DEPARTMENT OF ENERGY

ORNL/ATD--50

DE91 011215

DEVELOPMENT OF SENSORS FOR CERAMIC COMPONENTS IN ADVANCED PROPULSION SYSTEMS

D. L. Beshears
G. J. Capps

Applied Technology Division
Oak Ridge National Laboratory

H. M. Henson
T. L. Hatmaker
M. J. Bridges
R. S. Sadler-Sherles
B. S. Lankford

Technical Division
Oak Ridge K-25 Site

T. J. Henson

Metals and Ceramics Division
Oak Ridge National Laboratory

L. A. Zevenbergen

Chemical Technology Division
Oak Ridge National Laboratory

Prepared for NASA Lewis Research Center
Order No. C-30031-P

Date Published—November 1990

Prepared by the
Oak Ridge National Laboratory
and the
Oak Ridge K-25 Site
Oak Ridge, Tennessee 37831-7294
managed by
MARTIN MARIETTA ENERGY SYSTEMS, INC.
for the
U.S. DEPARTMENT OF ENERGY
under contract DE-AC05-84OR21400

CONTENTS

LIST OF FIGURES

ABSTRACT

This study, which was performed for the National Aeronautics and Space Administration-Lewis Research Center in conjunction with Pratt & Whitney, was undertaken to determine the feasibility of utilizing thermographic phosphors for monitoring the temperature of ceramic engine components above 1000° C. The Applied Technology Division of the Oak Ridge National Laboratory was asked to choose the appropriate phosphors and use existing technology to bond the phosphors to candidate substrates for future evaluation by Pratt & Whitney. The two high-temperature phosphors chosen were Y_2O_3:Eu and $Y_3(Al,Ga)_5O_{12}$:Tb. Utilizing existing technology for bonding high-temperature phosphors to nickel-based turbine blades, the phosphors were bonded to several different ceramic substrates. The ceramic substrates provided by Pratt & Whitney were silicon nitrate, silicon carbide, mullite, zirconia, and compglas. The phosphor/substrate system was cycled to 1500° C by Pratt & Whitney researchers. Surface characterization of a small number of phosphor/substrate systems was performed. The phosphor adherence was good on the majority of the samples. The phosphor/substrate system survived well for a first attempt at coating ceramic-based materials. Several samples showed evidence of either the phosphor diffusing into the substrate or the substrate material diffusing into the phosphor coating. Additional work is needed to optimize the phosphor/substrate system.

INTRODUCTION

Researchers at the Oak Ridge National Laboratory (ORNL) have experience in thermographic phosphor techniques for monitoring and analyzing high temperatures in highly erosive environments inside turbomachinery.[1-4] During the past five years, researchers at ORNL, in collaboration with researchers at Los Alamos National Laboratory and EG&G, Santa Barbara (also Department of Energy facilities), have performed research and development activities in the area of thermographic phosphors. This work has included screening of commercially available phosphors, manufacturing of special phosphors, calibration of various phosphors over a range of temperatures from 4 to 1673 K,[5,6] developing bonding techniques for bonding particular phosphors to a variety of substrates,[7,8] and performing laboratory and field experiments utilizing the thermal phosphors.

This study, performed for the National Aeronautics and Space Administration (NASA)-Lewis Research Center in conjunction with Pratt & Whitney, is entitled "Development of Sensors for Ceramic Components in Advanced Propulsion Systems." It is an initial investigation as to the feasibility of using thermographic phosphors for monitoring temperatures of ceramic components above 1000°C. ORNL researchers chose two appropriate high-temperature phosphors. Using existing technology for bonding high-temperature phosphors to nickel-based turbine blades, the phosphors were bonded to various ceramic materials. The ceramic materials provided by Pratt & Whitney were silicon nitrate (Si_3N_4), silicon carbide (SiC), mullite, zirconia, and compglas.

PHOSPHORS AND BONDING TECHNIQUES CHOSEN

Two phosphors, Y_2O_2:Eu and $Y_3(Al,Ga)_5O_{12}$:Tb (YAG:Tb), were chosen for the study because of their thermographic properties at elevated temperatures. Figure 1 shows the temperature dependency of these two phosphors as determined by EG&G Santa Barbara.[9] Decay-time data were collected at 611 and 543 nm for the phosphors Y_2O_2:Eu and YAG:Tb, respectively.

Two bonding techniques were used to apply Y_2O_2:Eu—electron-beam deposition and radio-frequency sputtering. All the YAG:Tb samples were coated using the electron-beam deposition technique. Seventy-three sample coupons were coated. Tables 1 through 3 summarize the 73 sample coupons in terms of the phosphor used, the coating process, the substrate materials used, and the sample code designation. Once the coupons were coated, a heat treatment was used to drive off contaminants, increase the relative intensity (signal level) of the phosphor coatings, and re-establish the typical fluorescent spectra. The heat treating and how it affects relative intensities will be discussed later in this report. For each substrate material, coating process, and phosphor type, a single sample coupon was maintained as a control, and the remaining samples were supplied to Pratt & Whitney for temperature-cycling evaluation.

Table 1. Summary of Y_2O_3: Eu sample coatings using electron-beam deposition

Phosphor coating	Coating process	Substrate material	Code designation	Relative intensity		
				As coated	Heat treated	After cycling
Y_2O_3:Eu			Standard	1.0	1.0	
	Electron-beam disposition	Zirconia	ZEB1	0.0101	0.10	
			ZEB2	0.0088	0.18	
			ZEB3	0.0091	0.21	0.134
			ZEB4	0.0055	0.14	
			ZEB5	0.0099	0.13	
		Mullite	MEB1	0.0097	0.26	0.002
			MEB2	0.0091	0.25	
			MEB3	0.0086	0.25	
			MEB4	0.0065	0.26	
			MEB5	0.0047	0.26	
		Compglas	CGEB1	0.0080	0.15	0.039
			CGEB2	0.0040	0.10	
			CGEB3	0.0040	0.07	
			CGEB4	0.0036	0.11	
			CGEB5	0.0042	0.14	
		Silicon carbide	SCEB1	0.0040	0.11	0.214
			SCEB2	0.0044	0.16	
			SCEB3	0.0032	0.13	
			SCEB4	0.0041	0.14	
			SCEB5	0.0040	0.15	
		Silicon nitrate	SNEB1	0.0038	0.17	
			SNEB2	0.0035	0.18	
			SNEB3	0.0040	0.19	0.052
			SNEB4	0.0038	0.20	
			SNEB5	0.0042	0.20	

Table 2. Summary of Y_2O_3: Eu sample coatings using RF sputtering

Phosphor coating	Coating process	Substrate material	Code designation	Relative intensity		
				As coated	Heat treated	After cycling
Y_2O_3:Eu			Standard	1.0	1.0	
	RF sputtering	Zirconia	ZRF1	0.0001	0.0086	0.009
			ZRF2	0.0001	0.0112	
			ZRF3	0.0001	0.0073	
			ZRF4	0.0000	0.0	
			ZRF5	0.0003	0.0073	
		Mullite	MRF1	0.0000	0.012	
			MRF2	0.0000	0.012	
			MRF3	0.0000	0.014	
		Compglas	CGRF1	0.0003	0.0094	
			CGRF2	0.0003	0.0086	
			CGRF3	0.0001	0.0086	
			CGRF4	0.0001	0.0077	
			CGRF5	0.0003	0.0094	
		Silicon carbide	SCSPY1	0.0003	0.0045	
			SCSPY2	0.0003	0.0062	0.014
			SCSPY3	0.0004	0.0049	
			SCSPY4	0.0003	0.0053	
			SCSPY5	0.0001	0.0058	
		Silicon nitrate	SNSPY1	0.0004	0.0066	
			SNSPY2	0.0003	0.70	
			SNSPY3	0.0005	0.0062	0.013
			SNSPY4	0.0001	0.0070	
			SNSPY5	0.0003	0.0066	

Table 3. Summary of YAG:Tb sample coatings using electron-beam deposition

Phosphor coating	Coating process	Substrate material	Code designation	Relative intensity		
				As coated	Heat treated	After cycling
YAG:Tb			Standard	1.0	1.0	
	Electron-beam deposition	Zirconia	ZYT1	0.0013	0.49	
			ZYT2	0.0007	0.54	
			ZYT3	0.0006	0.56	
			ZYT4	0.0005	0.54	0.021
			ZYT5	0.0006	0.50	
		Mullite	MYT1	0.0013	0.57	
			MYT2	0.0002	0.51	
			MYT3	0.0007	0.59	
			MYT4	0.0006	0.60	
			MYT5	0.0006	0.53	
		Compglas	CYT1	0.0013	0.28	
			CYT2	0.0013	0.28	
			CYT3	0.0009	0.43	
			CYT4	0.0009	0.0049	
			CYT5	0.0003	0.06	
		Silicon carbide	SCYT1	0.0031	0.37	
			SCYT2	0.0009	0.39	
			SCYT3	0.0009	0.25	
			SCYT4	0.0007	0.33	
			SCYT5	0.0008	0.42	
		Silicon nitrate	SNYT1	0.0005	0.17	
			SNYT2	0.0006	0.47	0.006
			SNYT3	0.0005	0.22	0.012
			SNYT4	0.0005	0.18	
			SNYT5	0.0007	0.19	

Prior to coating, each sample coupon was cleaned with acetone. The Si_3N_4 and SiC coupons were extremely smooth, making it was difficult to adhere to the surface. A reverse sputtering process was used on each of the Si_3N_4 and SiC coupons to remove contaminants and roughen the surface prior to cleaning. This improved the adherence considerably, and in the future, this will be standard practice for all ceramics materials.

HEAT TREATING FOR IMPROVED SIGNAL LEVELS

In working with the electron-beam-deposited and RF-sputtered coatings for the nickel-based alloys, it was found that heat treating the as-coated samples was required. The heat-treating process served to drive off surface contamination, increase the signal intensity, and re-establish the fluorescent spectral signature of the phosphor in question. To determine if heat treating would be required, a fluorescent spectra was run on each of the as-coated samples. The signal intensity and spectral structure of each of the samples was compared with those of a standard hot-pressed pellet of the phosphor material. Both the electron-beam and the RF-sputtered as-deposited samples exhibited spectra that were significantly different than the pressed pellet. In addition, the signal intensity, in most cases, was down by a factor of more than 100. The sample coupons were then heat treated at 950° C for 3 h, and the fluorescent spectra was repeated. The surface chemistry analysis of an as-coated sample compared with a heat-treated sample showed that the heat treating caused a complete change in the surface morphology. The surface concentration of carbon dropped during the heat-treating cycle. The heat-treating process again served to drive off contaminants, increase the relative intensity, and re-establish the typical fluorescent spectra. Figure 2 shows a typical spectra for a Y_2O_2:Eu standard hot-pressed pellet. Figure 3 shows a typical as-deposited and after-heat-treating spectra for electron-beam-deposited Y_2O_2:Eu. Figure 4 shows a typical spectra for a YAG:Tb standard hot-pressed pellet. Figure 5 gives a typical as-deposited and after-heating spectra for an electron-beam-deposited YAG:Tb sample. To fully understand the heat-treating process, additional time and funding would be required, which is beyond the scope of this program. The columns in Tables 1 through 3 labeled Relative Intensity, As Coated, and Heat Treated refer to the relative intensity (signal level of the temperature-dependent line of interest—in this case, the 611-nm line for Y_2O_3:Eu and 544 nm for the YAG:Tb) of the samples when compared with a standard hot-pressed pellet of the appropriate phosphor. As can be seen, the signal intensity is greatly increased by heat treating the samples. The last column in Tables 1 through 3 gives the resulting relative intensity of several samples after Pratt & Whitney temperature cycling to either 1400 or 1500° C.

SURFACE CHARACTERIZATION OF THE THERMOGRAPHIC PHOSPHORS

Funding levels only allowed a small amount of surface characterization to be performed. Surface characterization was performed using the scanning electron microscope (SEM), energy-dispersive (EDS) X-ray analysis, electron-microprobe analysis, backscattered electron imaging, and X-ray photoelectron spectroscopy.

The surface characterization was performed on four samples. The samples chosen were all coated with YAG:Tb phosphor using the electron-beam deposition. The first set of samples chosen was Si_3N_4 substrates SNYT5 (the control sample that was coated and heat treated and no additional temperature cycling performed) and SNYT3 (one of the four samples that was temperature cycled to 1500°C by Pratt & Whitney). The second set of samples chosen was zirconia (ZrO^2) substrates ZYT5 (the control sample that was coated and heat treated at 950°C and no additional temperature cycling performed) and ZYT3 (one of the four samples that were temperature cycled to 1500°C by Pratt & Whitney).

YAG:Tb ELECTRON BEAM DEPOSITED ON Si_2N_4SUBSTRATE

Fluorescence intensity of the coating dropped by an order of magnitude after thermal cycling to 1500°C (see Table 3). The thermal-cycled coupon showed obvious morphological damage as shown in Fig. 6.

Figure 7 compares the coated surface after heat treatment at 950°C with a similar surface after thermal cycling. The heat-treated surface was covered with a network of thermal cracks and had some regions beginning to show signs of flaking. After thermal cycling, two discrete surfaces were observed. The center of the Si_3N_4 coupon contained a thick region of bubbled coating, while the coupon edges were bare Si_3N_4 substrate. The original coating structure was destroyed during cycling, apparently due to the substrate Si diffusing to the surface and creating a puddling of the phosphor coating.

EDS analysis of the material present at the center of the coupon after thermal cycling is presented in Fig. 8. Y, Al, Ga, and Tb are still present in the coating. The coating contains Si as its major constituent. The surface is very irregular.

Electron microprobe examination (Fig. 9) of the thermally cycled coupon shows the coating components restricted to the surface. There is no evidence of any phosphor components diffusing into the substrate. However, the coating was confirmed to contain large amounts of Si, indicating that the Si did diffuse into the phosphor coating. The resultant coating microstructure is shown in Fig. 10. Backscattered electron imaging of the substrate indicates the presence of many metal particulates such as tungsten, iron and nickel.

In summary, substrate Si was incorporated into the phosphor coating, with subsequent melting.

YAG:Tb ELECTRON BEAM DEPOSITED ON A ZrO_2 SUBSTRATE

The thermal-cycled coating/substrate system showed little evidence of damage (Fig. 11). The fluorescent intensity again decreased by an order of magnitude after thermal cycling, as indicated in Table 3.

Coating surfaces of the YAG:Tb/ZrO_2 system are compared in Fig. 12 before and after the thermal cycle. Some surface texture appears to have developed during cycling. EDS analysis of these surfaces indicates a loss of surface Tb (as well as Cr coating contamination) during cycling (Fig. 13). This is confirmed by XPS surface (top 50 Å) analyses displayed in

Figs. 14a and 14b. While only very small amounts of Tb are present in the top 50 Å before thermal cycling, none is detectable afterward. Intensity ratios for the YAG components (Y:Al:Ga) were 6:1:3 after heat treatment and 3:1:6 after thermal cycling, showing preferential diffusion into the substrate. The surface depletion of the fluorescent component of the phosphor has been observed on both electron beam and sputtered coatings. Correlation of elemental distribution within the coatings with fluorescent performance could potentially offer significant performance improvement.

Electron microprobe scanning images (Figs. 15 and 16) demonstrate how the coating components have diffused into the zirconia substrate. Both the Tb and the Y diffusion is evident; Ga remains in the coating. It appears that the incorporation of a diffusion barrier into the phosphor/substrate system may expand the useful range of this phosphor system.

SUMMARY OF RESULTS AND RECOMMENDATIONS

Overall the phosphor/substrate systems survived well for a first attempt at coating ceramic based materials. The phosphor adherence was good on most of the samples. In most cases, the phosphor performed as well as or better than the substrate materials. In most cases, where the phosphor performance was, poor it was due to substrate degradation. Several samples showed evidence of either the phosphors diffusing into the substrate material or the substrate material diffusing into the phosphor coating. Details of how this affected the phosphor's intensity and thermometry characteristics were beyond the scope of this program and therefore not addressed. Although the phosphor intensity or signal levels decreased by an order of magnitude after thermal cycling, they still remained at a level adequate to perform thermal diagnostics. A next step in evaluating and improving the phosphor/substrate systems would include the following:

1. Incorporate a diffusion barrier into the phosphor/substrate system to prevent both the diffusion of phosphor components into the substrate and the diffusion of the substrate materials into the phosphor coatings;

2. Incorporate a reverse sputtering step into the cleaning and sample preparation phase for all ceramic materials to improve the adherence of the phosphor to the ceramic substrates;

3. Determine the effect of surface depletion of the fluorescent component on the signal level performance by correlatingthe elemental distribution with the coating fluorescent performance;

4. Optimize the deposition parameters for the various substrates to maximize both coating durability and fluorescent intensity;

5. Screen substrate materials as to their suitability for high temperature integrity;

6. Perform basic research to qualify new potential phosphors candidates for applications above 1500° C. Included would be theoretical considerations of phosphor fluorescence mechanism and calibration of candidate materials.

7. Evaluate surface and interface contamination, either from surface materials or during processing. This can alter both fluorescence and adherence characteristics. Surface analyses of substrate and coating surfaces could offer valuable information for describing and monitoring process steps.

REFERENCES

1. B. W. Noel et al., "Evaluating Thermographic Phosphors in an Operating Turbine Engine," 1990 ASME Turbo Expo - Land, Sea and Air, Brussels, Belgium, June 11-14, 1990, ASME Paper 90-GT-266.

2. A. R.Bugos et al., "Emission Properties of Phosphors for High Temperature Sensor Applications," Proc. IEEE Southeastcon Conference, Knoxville, TN, April 10-13, 1988.

3. K. W. Tobin et al., "Remote High-Temperature Thermometry of Rotating Test Blades Using YVO_4:Eu and Y_2O_3:Eu Thermographic Phosphors," AIAA/ASME/SAE/ASEE 24th Joint Propulsion Conference, Boston, Massachusetts, AIAA-88-3147, July 11-13, 1988.

4. B. W. Noel et al., *Thermographic-Phosphor Temperature Measurements in Turbine Engines: Program Review, 1986*, LA-UR-87-979, Los Alamos Natl. Lab., Los Alamos, NM, March 1987.

5. D. L. Beshears, "Laser-Induced Fluorescence of Phosphors for Remote Cryogenic Thermometry," SPIE OE/FIBERS '90 Sensors, Networking, and Communications, San Jose, California, September 16-21, 1990.

6. C. M. Simmons, *Low-Temperature Phosphor Thermometry: Calibration of Europium-Doped Lanthanum Oxysulfide Between Room Temperature and -194 °C*, ORNL/ATD-25, Martin Marietta Energy Systems, Inc., Oak Ridge Natl. Lab., February 1990.

7. D. L. Beshears et al., *Phosphor Bonding Studies - Burner Rig Endurance Test*, K/ETAC-59, Martin Marietta Energy Systems, Inc., Oak Ridge Nat. Lab., July 1988.

8. D. L. Beshears, M. J. Bridges, and L. A. Harris, *Evaluation of Commercially Available Coating Techniques for Application of Thermographic Phosphor to Nickel Based Alloys*, K/TS11,801, Martin Marietta Energy Systems, Inc., Oak Ridge Gaseous Diffusion Plant, April 1986.

9. W. Lewis et al., "Noncontact Thermometry in Excess of 2500 °F Using Thermographic Phosphors," ISA Proceedings 1990, ISA, 1990, Paper 90-103.

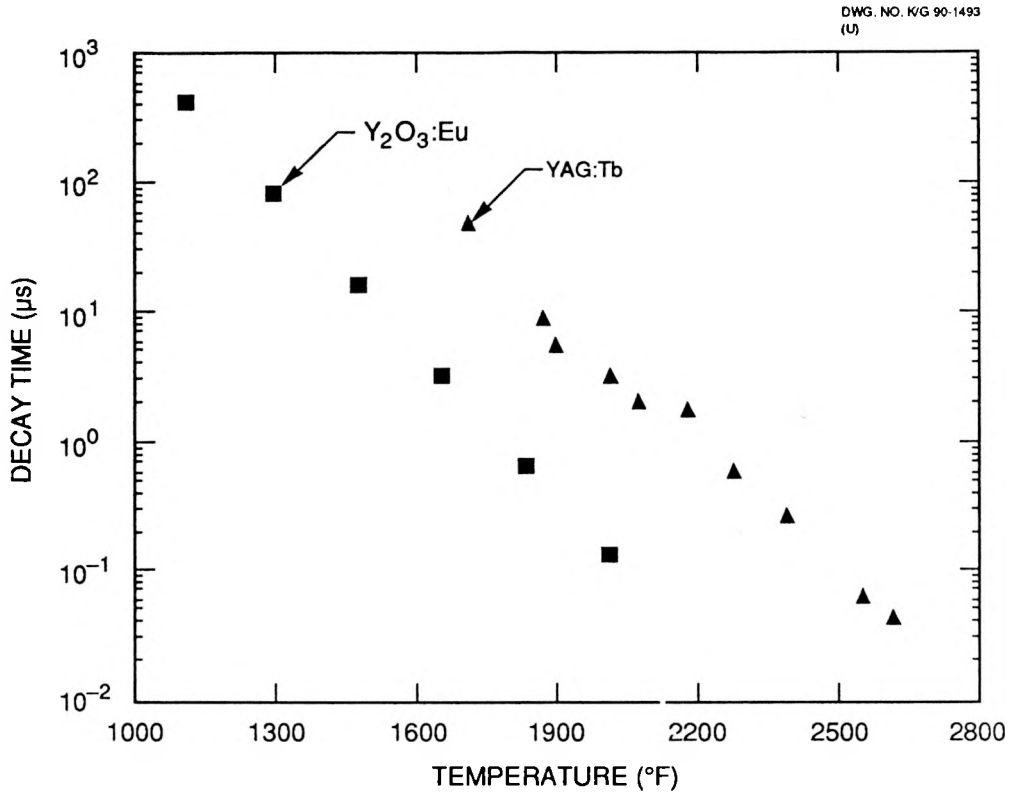

Fig. 1. Decay times for Y_2O_3:Eu and YAG:Tb as a function of temperature.

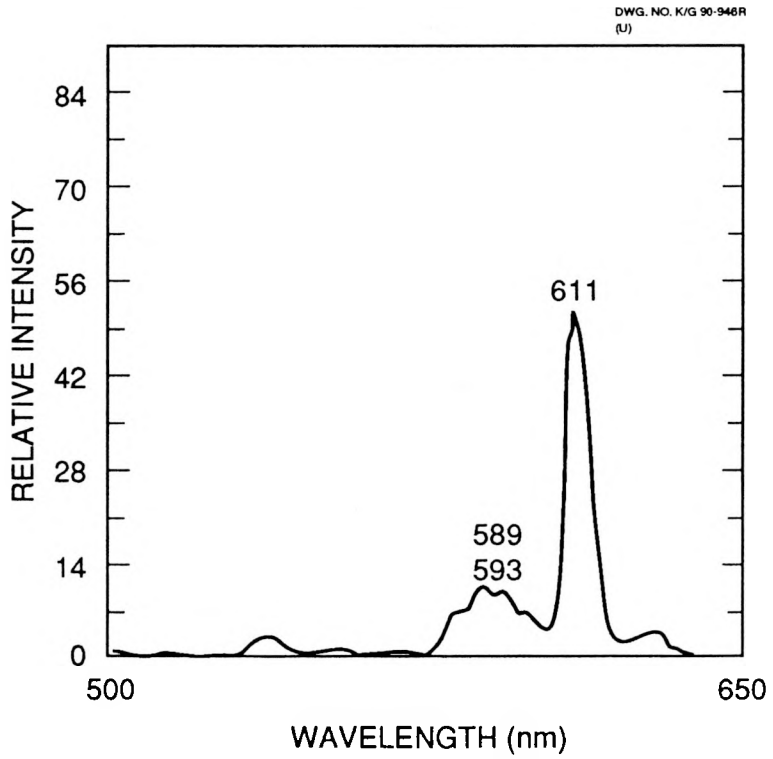

Fig. 2. Emission spectra for Y_2O_3:Eu pressed-pellet standard. Excitation λ - 266 nm.

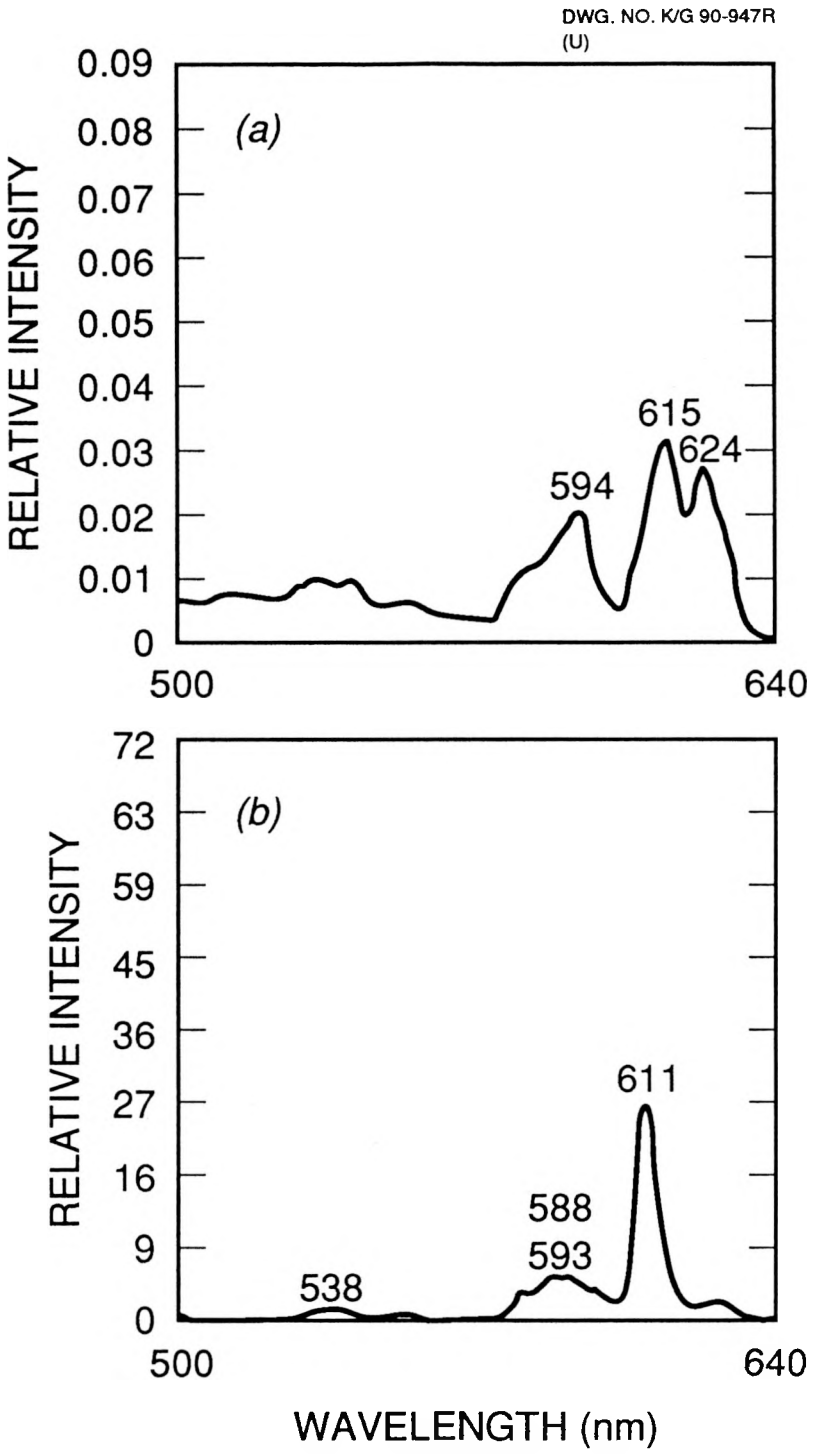

Fig. 3. Emission spectra for Y_2O_3:Eu electron beam deposited on mullite. *(a)* as deposited, *(b)* heat treated at 950°C for 3 h. Excitation λ - 265 nm.

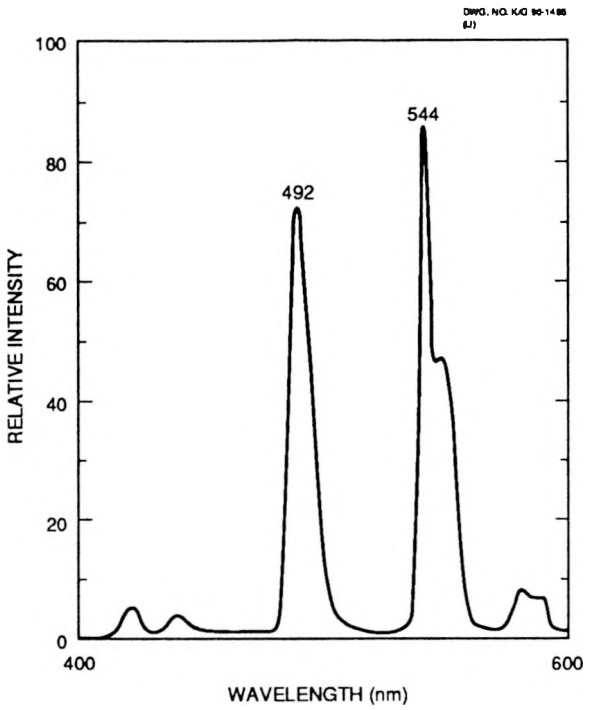

Fig. 4. Emission spectra for YAG:Tb pressed pellet standard. Excitation λ - 265 nm.

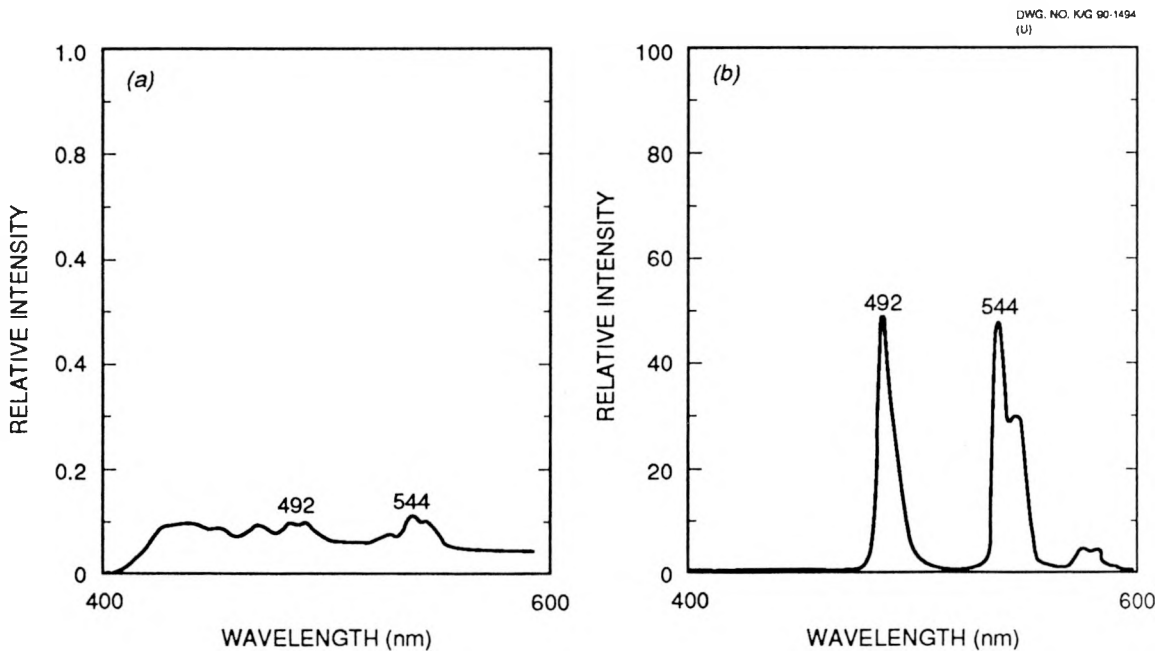

Fig. 5. Emission spectra for YAG:Tb electron beam deposited on mullite. *(a)* As deposited, *(b)* heat treated at 950°C for 3 h. Excitation λ - 265 nm.

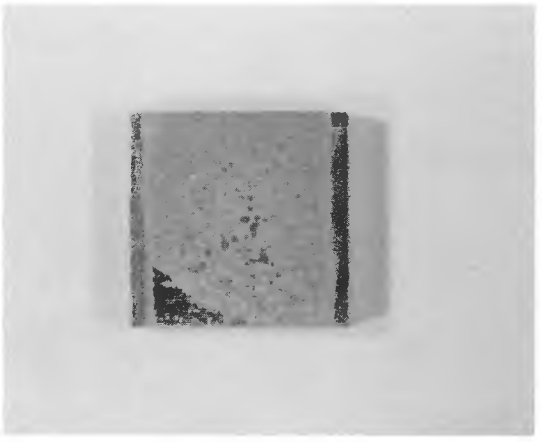

Heat treated at 950°C

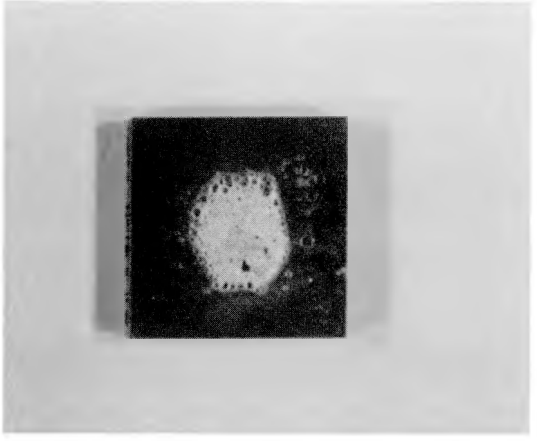

Thermally cycled at 1500°C

Fig. 6. YAG:Tb/silicon nitrate electron-beam deposition.

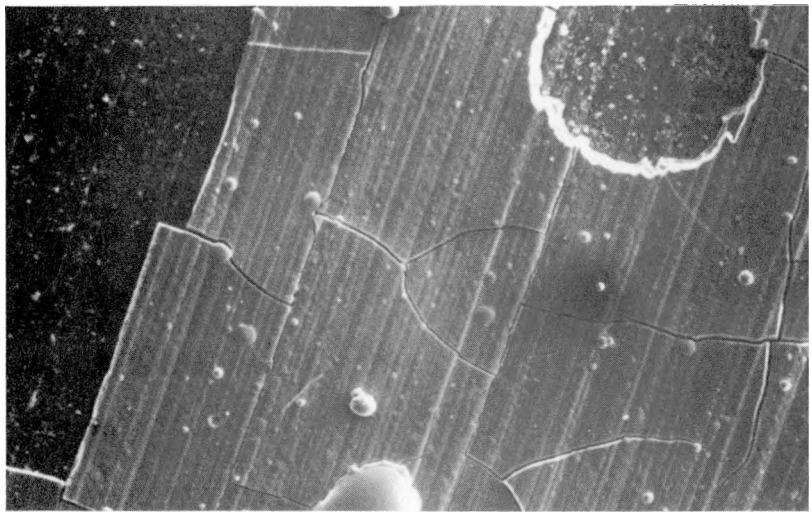

950°C heat treatment

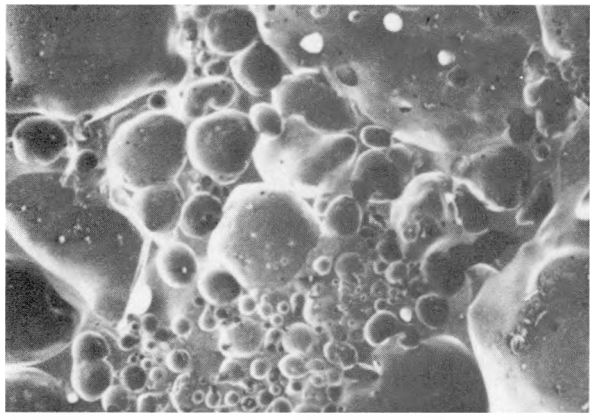

After thermal cycling to 1500°C - center region

After thermal cycling to 1500°C - edge region

Fig. 7. YAG:Tb/silicon nitrate SEM (100X).

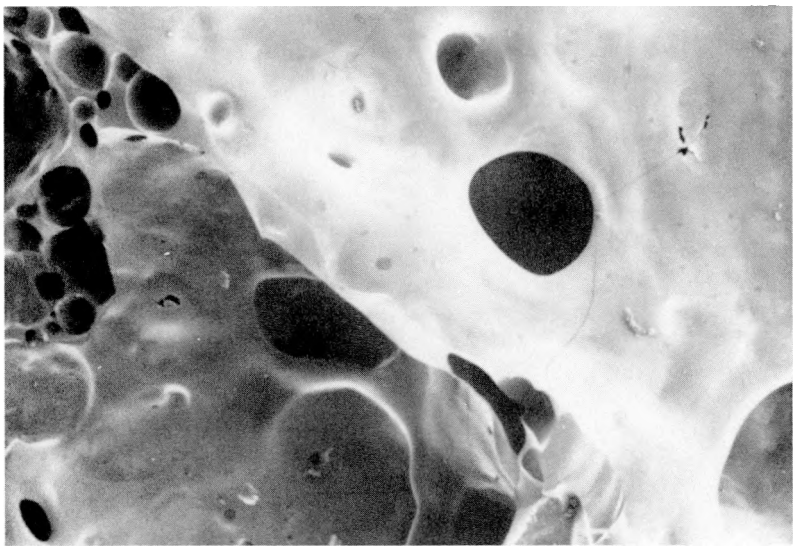

(a) Surface morphology (SEM - 100X).

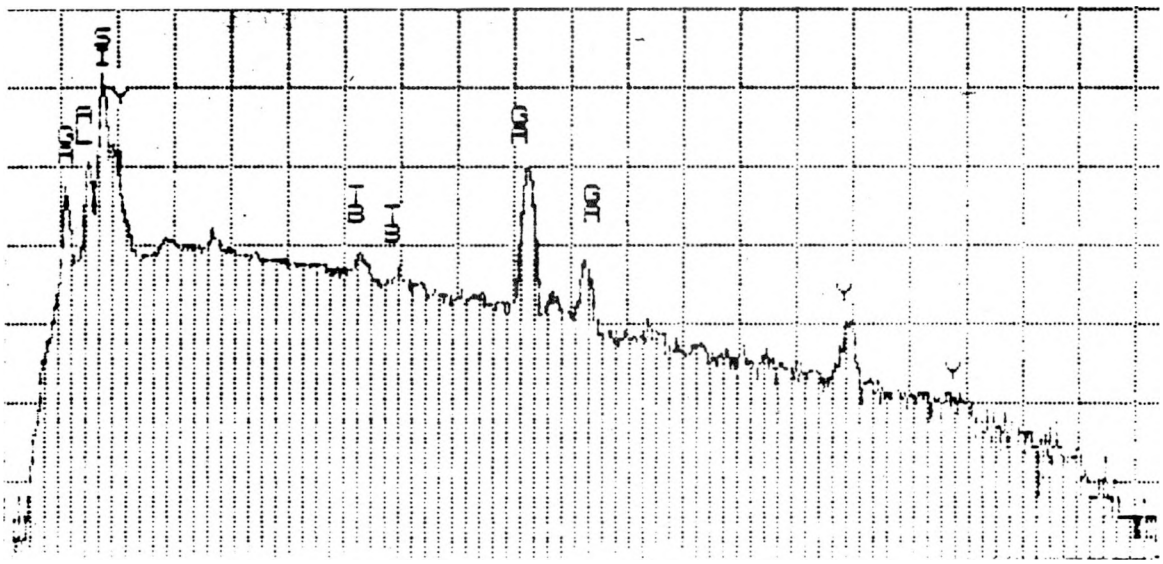

(b) Energy-dispersive x-ray analysis of surface.

Fig. 8. YAG:Tb/silicon nitrate. Coating morphology and anlaysis after thermal cycling to 1500°C.

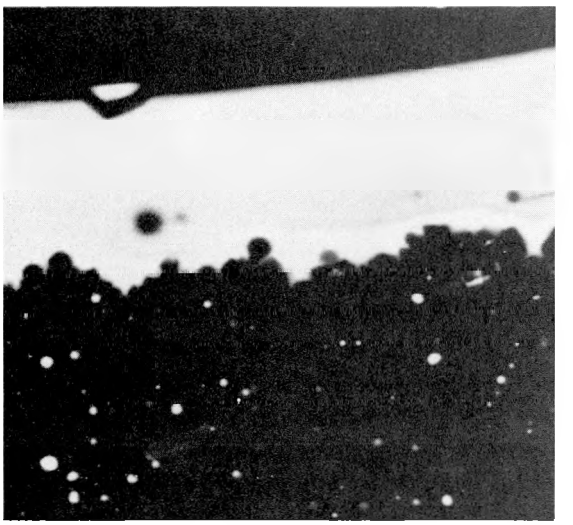

Backscattered electron

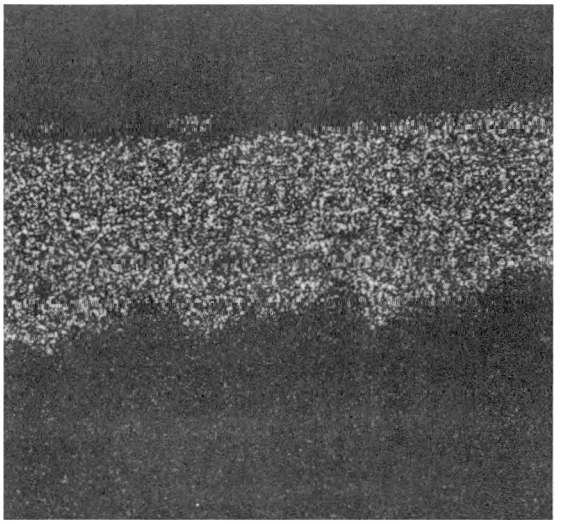

TbLα

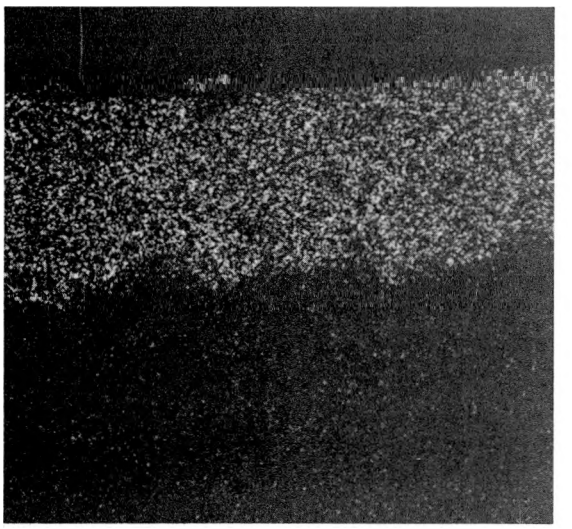

YLα

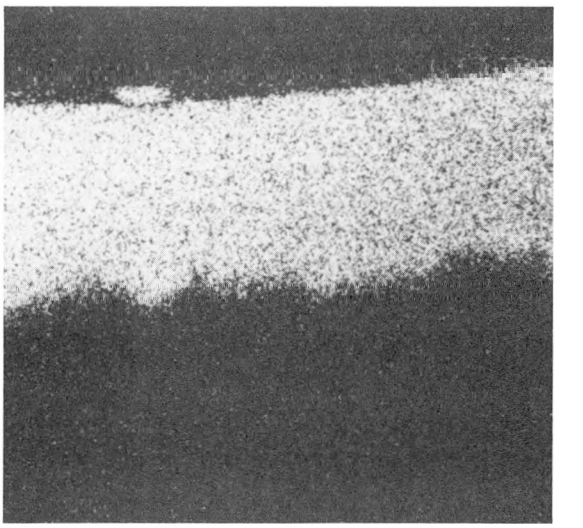

GaKα

Fig. 9. YAG:Tb/silicon nitrate. Electron-microprobe-scanning images of coating/substrate interface after thermal cycling at 1500°C (860X).

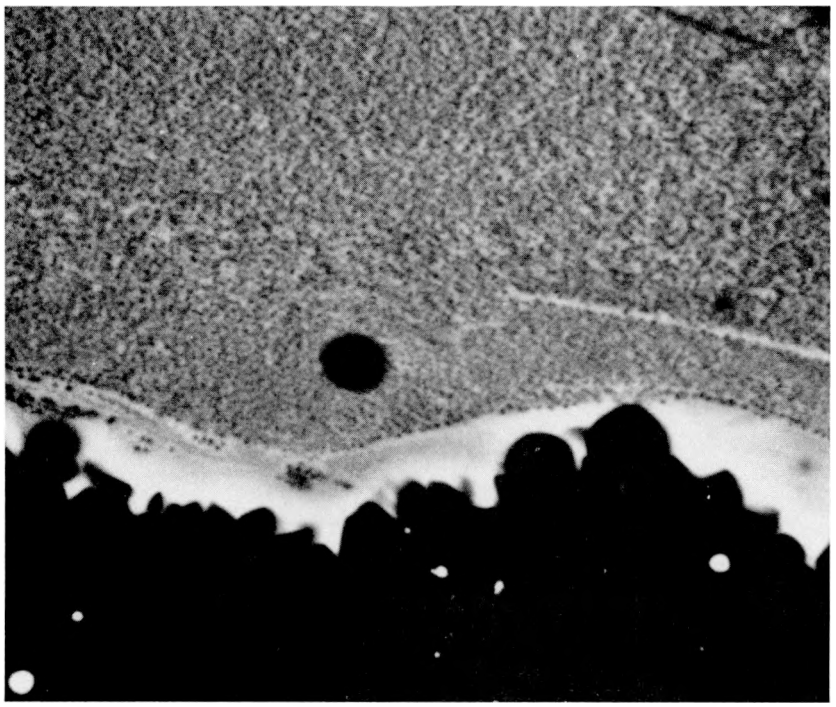

Fig. 10. YAG:Tb/silicon nitrate. Electron-microprobe-scanning image of coating after thermal cycling at 1500°C (2400X).

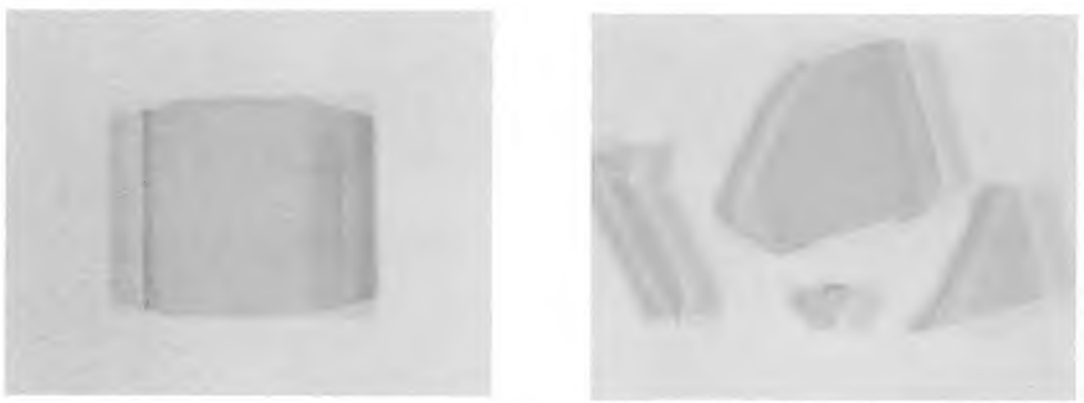

Heat treated at 950°C

Thermally cycled to 1500°C

Fig. 11. YAG:Tb/zirconia electron-beam deposition.

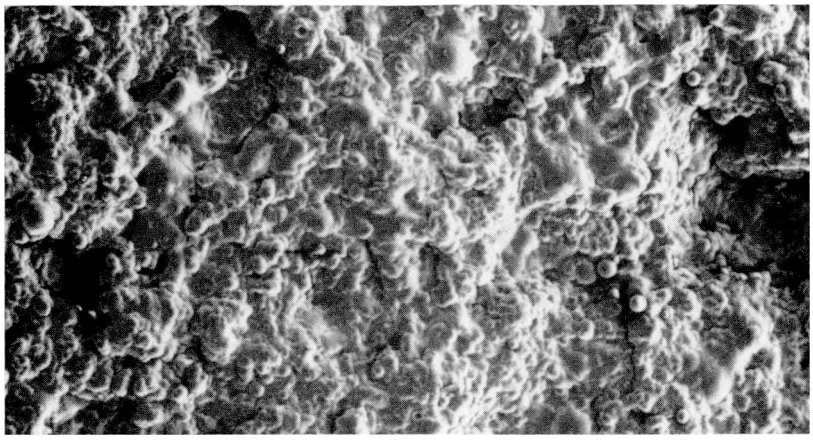

(a) 950°C heat treatment.

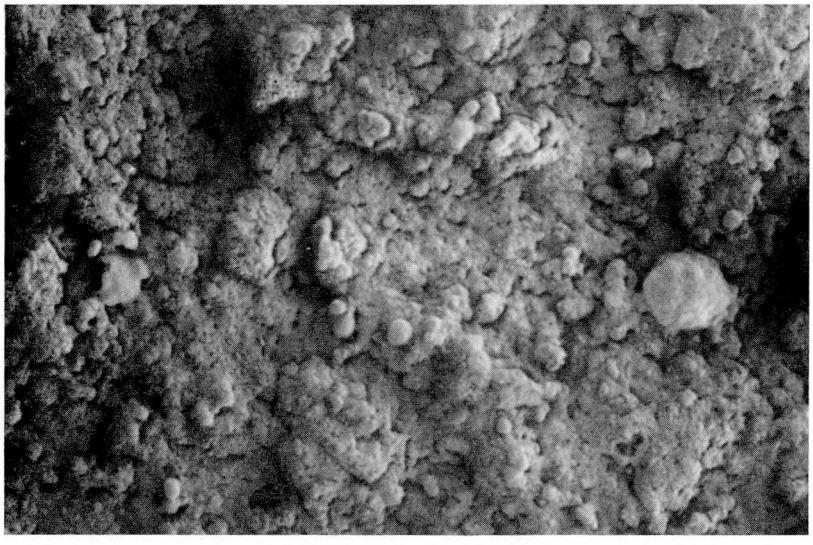

(b) After thermal cycling to 1500°C.

Fig. 12. YAG:Tb/zirconia SEM (100X).

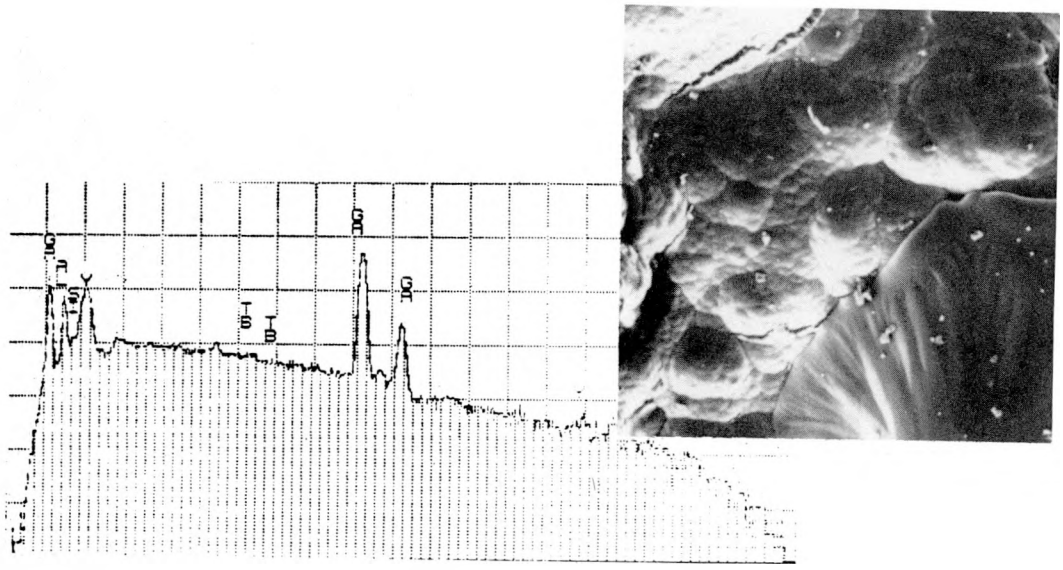

950°C heat treatment (1000X)

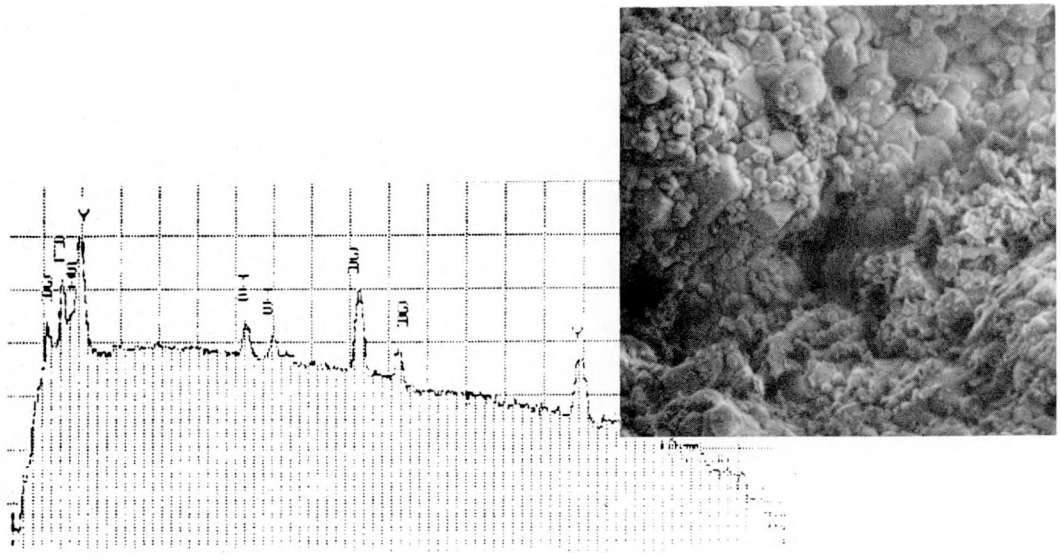

After thermal cycling to 1500°C (1000X)

Fig. 13. YAG:Tb/zirconia. Coating morphology and analysis.

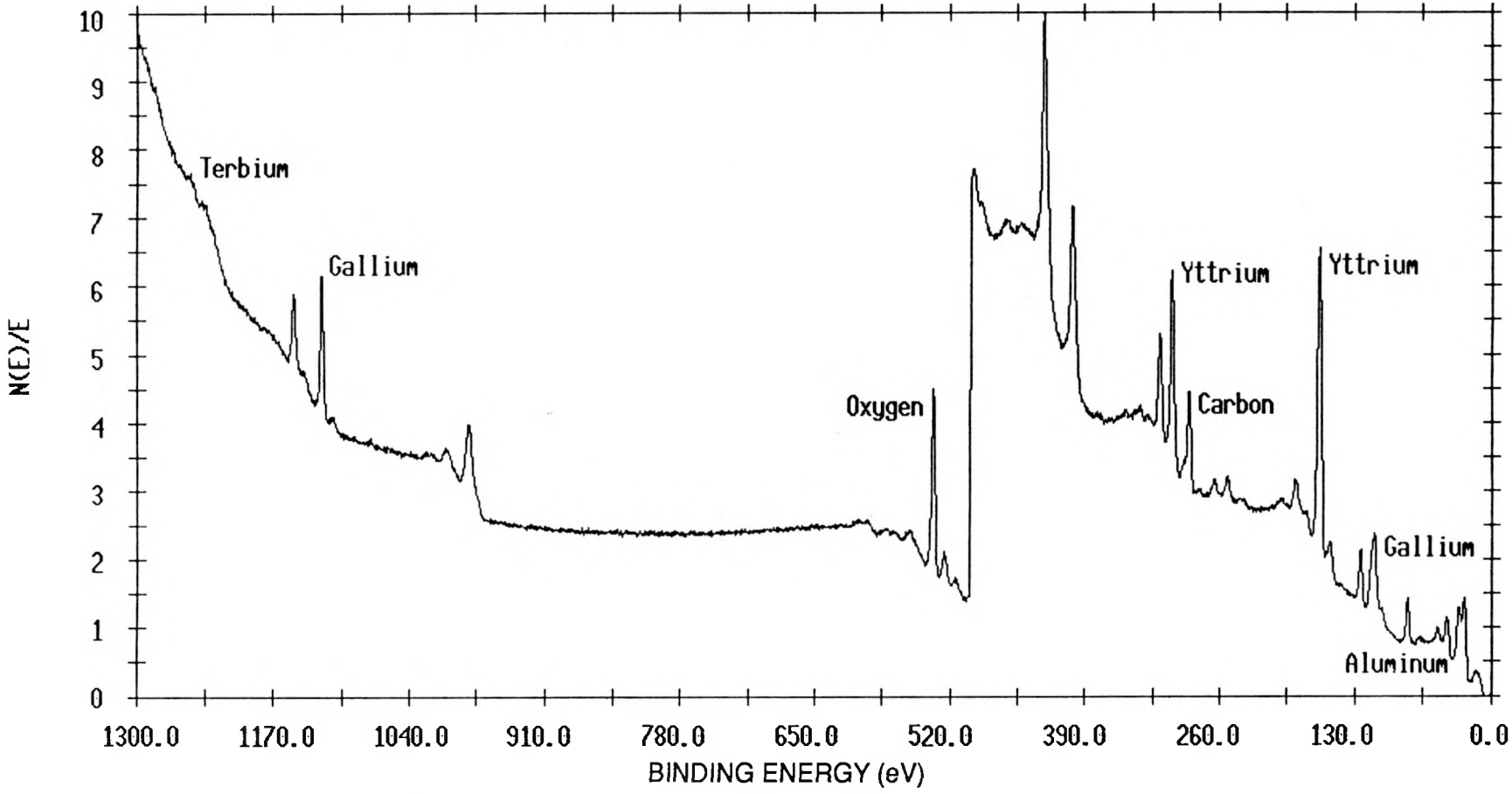

Fig. 14a. YAG:Tb/zirconia heat treated at 950°C. XPS surface analysis.

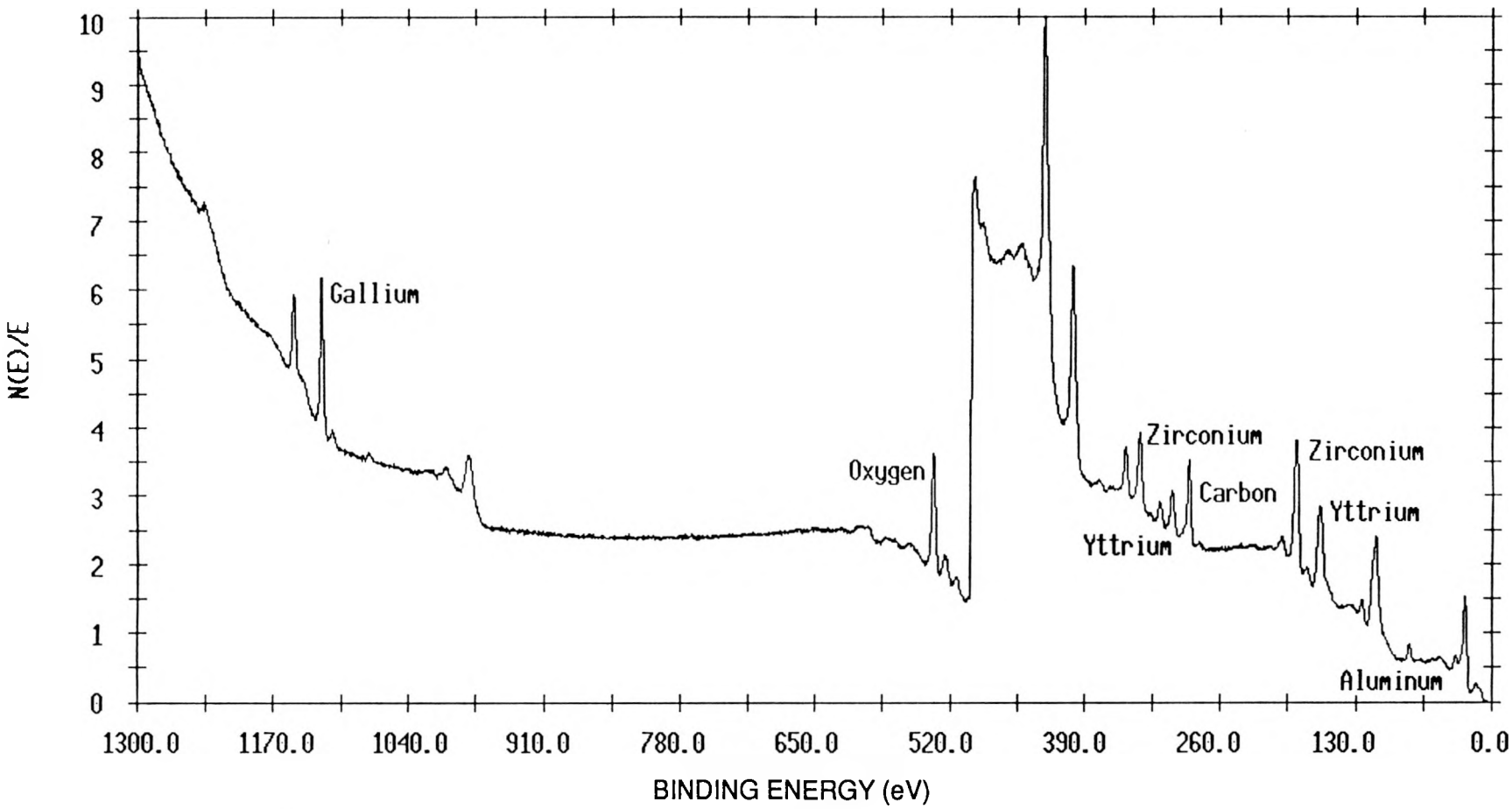

Fig. 14b. YAG:Tb/zirconia thermally cycled to 1500°C. XPS surface analysis.

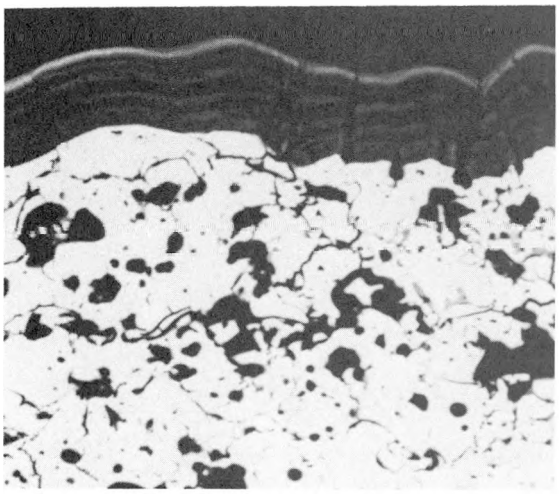

Backscattered electron

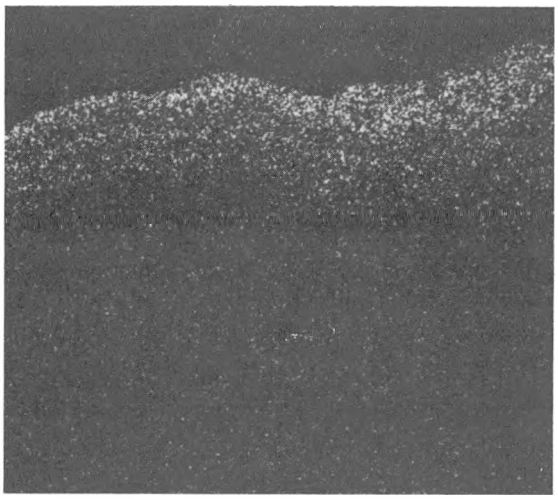

TbLα

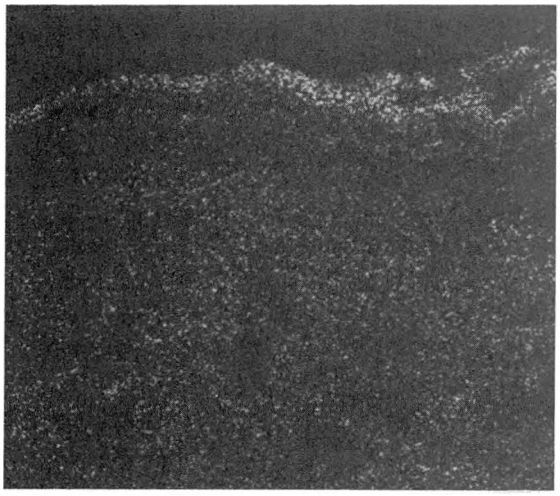

YLα

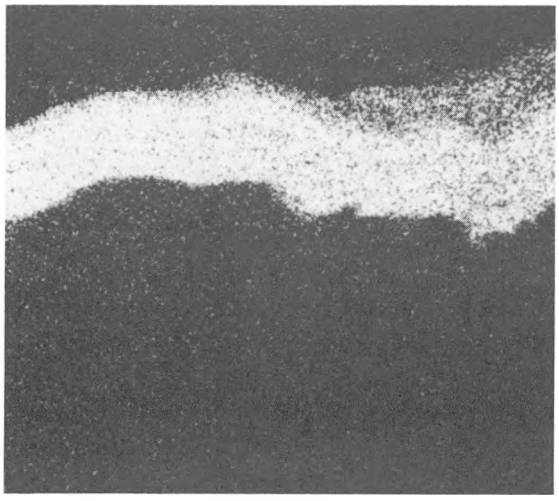

GaKα

Fig. 15. YAG:Tb/zirconia. Electron-microprobe-scanning images of coating/substrate interface after thermal cycling at 950°C (600X).

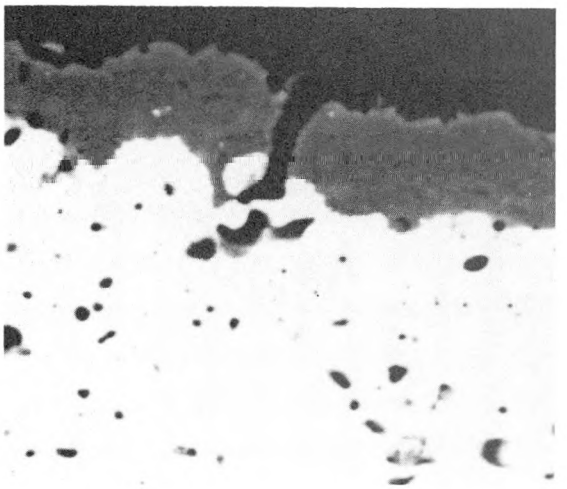

Backscattered electron

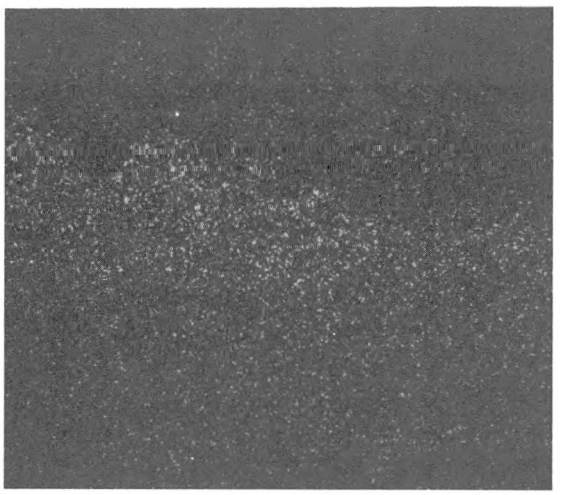

TbLα

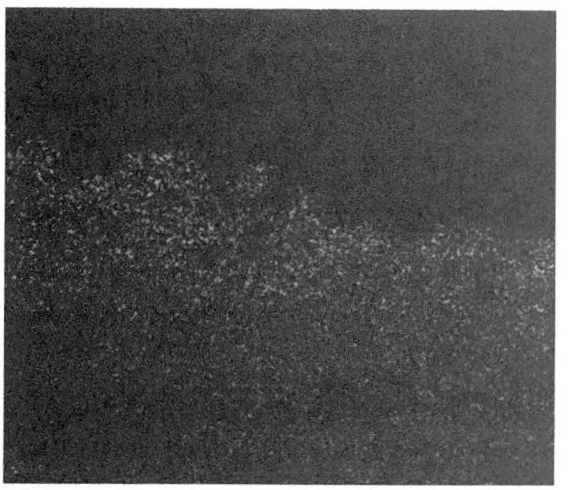

YLα

GaKα

Fig. 16. YAG:Tb/zirconia. Electron-microprobe-scanning images of coating/substrate interface after thermal cycling at 1500°C (860X).

Internal Distribution

1-6. D. L. Beshears
7. M. L. Bridges
8-10. G. J. Capps
11. M. R. Cates
12. J. B. Dooley
13. H. M. Henson
14-15. T. J. Henson
16. T. L. Hatmaker
17. J. G. Hubrig
18. W. S. Key
19. B. S. Lankford
20. R. S. Sadler-Sherles
21. D. A. Waters
22. L. A. Zevenbergen
23. Applied Technology Library
24. Central Research Library
25. Y-12 Technical Library
26. ORNL Patent Section
27-28. Laboratory Records Department
29. Laboratory Records Department - RC

External Distribution

30-35. M. R. Cyr, Pratt & Whitney, 400 Main Street, East Hartford, Connecticut 06108
36. D. Chin, United Technologies, 400 Main Street, East Hartord, Connecticut 06108
37-42. R. Holanda, NASA Lewis Research Center, MS 7791, 21000 Brookpart Road, Cleveland, Ohio 44135
43. J. Harris, NASA Lewis Research Center, MS 500-305, 21000 Brookpart Road, Cleveland, Ohio 44135
44. Assistant Manager, Energy Research and Development, U.S. Department of Energy, Oak Ridge Operations, P.O. Box 62, Oak Ridge, Tennessee 37831
45-46. Office of Scientific and Technical Information, P.O. Box 2001, Oak Ridge, Tennessee 37831